Making Stuff Glow

Thermally Activated Delayed Fluorescence in Synthetic Macrocyclic Anion Receptors

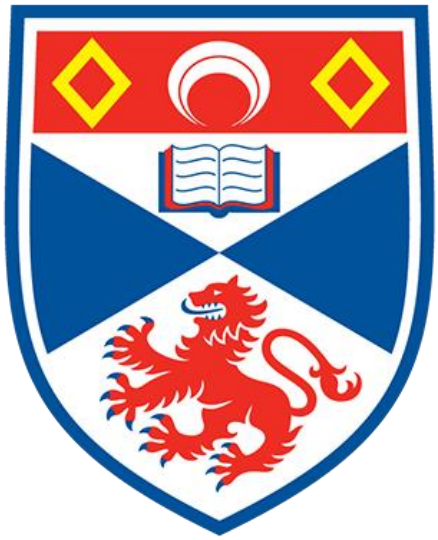

University of
St Andrews

Matthew Fry

with supervision from Professor Eli Zysman-Colman

LAIDLAW
SCHOLARS

INTRODUCTION

The ubiquity and prominence of anions in both biological and chemical systems justifies the pursuit of ever more sophisticated methods for their detection. Supramolecular chemistry has much to offer the field of anion recognition and macrocycles constitute a clear vehicle for this. Although, it should be mentioned that the application of these compounds reaches much further, including catalysis, possibly medical treatment, and anion sequestration from radioactive waste.[1] Several examples of these anion-binding large ring systems are known, however many rely on classical hydrogen bonds between the central anion and highly polarised, endocyclic $^{\delta+}$H-X$^{\delta-}$ bonds (X = N,O) as seen in *Figure 1.*[2] Whilst effective, these types of macrocycles are limited to organic, typically non-polar solvents, where there is little competition to the desired hydrogen bonding interaction, limiting their applicability in real-world contexts.[1]

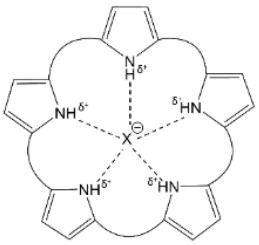

Figure 1: Classical H-bonded macrocycle

Thanks to the work of Bryantsev and Hay,[3] it was suggested that C-H bonds can play a meaningful role in anion binding, if sufficiently activated by neighbouring electron withdrawing groups. This was confirmed by Li and Flood,[2] when strong anion binding was observed in a neutral macrocycle (*Figure 2*) that operates exclusively *via* aromatic $^{\delta-}$C-H$^{\delta+}$ based H-bonds. The high electronegativity of the N atoms in the triazole rings activates the internal C-H bonds sufficiently for strong chloride binding. In line with predictions from Cram,[4] it appears that whilst the polarity of the relevant bonds is important to anion binding, preorganization and desolvation of these hydrogen-bond donor sites is also critical to the formation of stable complexes.

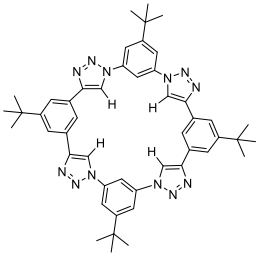

Figure 2: Macrocycle taken from literature[2]

The macrocycle shown in *Figure 2* and its synthesis were pivotal in the development of this project. Using it as a scaffold allowed for a new carbazole substituent to be appended, and the geometry of the resulting species, as well as its luminescence potential, to be estimated. This was done *via* Density Functional Theory, using the PBE0 functional and 6-31G(d,p) basis set, a well-established methodology in the EZ-C group. The results were encouraging, revealing an excited singlet-triplet state energy difference (ΔE_{ST}) of 0.15 eV, which is well within the bounds for thermally activated delayed fluorescence (TADF). Furthermore, the synthesis of the compound taken from the literature is comprised of well-known and reliable reactions, which can still be employed here. The aim of the project reported herein was to synthesise and characterise the target compound (TC), shown in *Figure 3*.

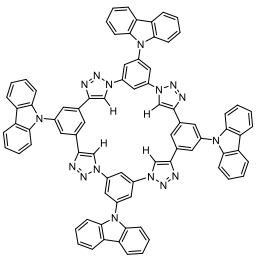

Figure 3: Target compound

The family of macrocycles synthesised by Li and Flood are not emissive, which limits their usefulness for sensing applications. Incorporation of carbazole units into the TC adds the value of photoluminescence, which increases its viability as a chemical sensor. The emission of the TC is largely attributable to fluorescence, which occurs from the lowest energy excited singlet state, in accordance with Kasha's rule.[5] It is a radiative decay process, whereby an electron relaxes back to its ground state without a change in spin. Quantum mechanically, this is a highly probable, allowed transition, meaning that the excited state is incredibly short-lived, and emission occurs on a nanosecond timescale. TADF is a special case of fluorescence, which is predicated on the up-conversion of non-emissive triplet states to emissive singlet states using the thermal energy of the molecule,[6] as illustrated in *Figure 4*. For this reverse intersystem crossing (RISC) from the triplet state up to the corresponding singlet state to be fast enough to be practically useful, ΔE_{ST} must be small (less than 0.3 eV) to ensure good mixing

of the singlet and triplet states. Given that ΔE_{ST} is governed by the exchange energy, which is related to spatial overlap, of the highest occupied molecular orbital (HOMO) and the lowest unoccupied

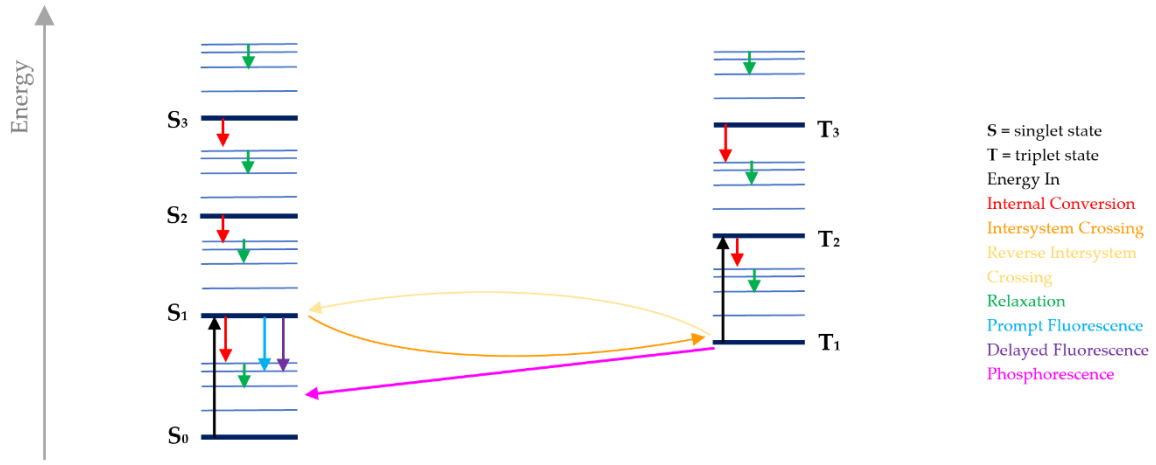

Figure 4: Jablonski diagram illustrating processes involved in prompt fluorescence, phosphorescence and TADF

molecular orbital (LUMO), it can be supressed by geographically confining the HOMO and LUMO to different regions of the molecule.[6] This explains the popularity of donor-acceptor systems containing a twisted bond in TADF literature; the twist brings the HOMO and LUMO out of alignment and reduces the ΔE_{ST}. These twisted bonds often come from increasing the steric bulk around the donor and acceptor moieties; here carbazole groups have been used to enforce this non-planarity. DFT computation of the TC in the gas phase suggests a HOMO residing over one of the donor groups and a LUMO situated over a portion of the macrocycle itself, as seen in *Figure 5,* indicating TADF potential.

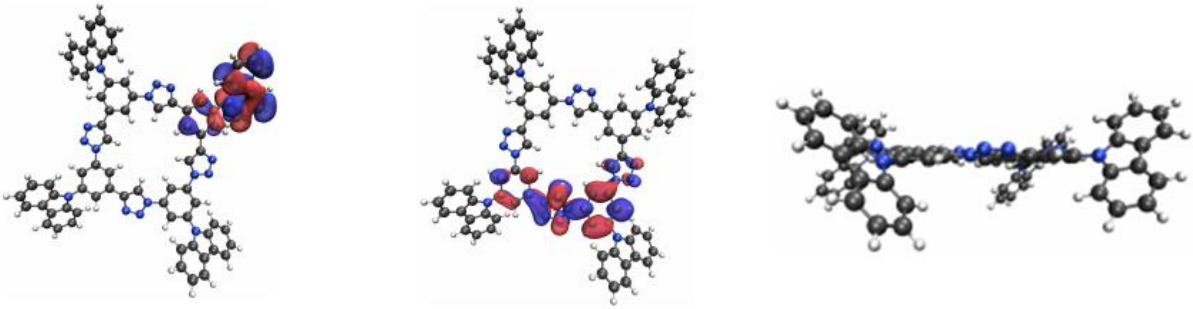

Figure 5a: HOMO residing on a donor carbazole group, 5b: LUMO residing over a part of the central macrocyclic acceptor, 5c: non-planarity of TC enforced by steric bulk of carbazole substituents.

TADF was revolutionised by advances in molecular design, with a plethora of synthetic possibilities enabling a variety of substituents to be incorporated into these entirely organic frameworks.[7] Depending on the electron donating/accepting ability of these substituents, the orbital energies can be tuned, giving access to TADF materials of many different colours. Furthermore, it is also possible that varying these substituents could lead to macrocycles which bind neutral molecules as well as anions, such as 1,3,5-trinitrotoluene (TNT), broadening the scope of their application.[8]

There are many examples of fluorescent anion receptors whose luminescence behaviour varies on anion binding. [1] The changes in optical properties (such as colour or intensity) of emissive macrocycles when they form complexes with anions is what makes them so useful as receptors. Given the large proportion of total fluorescence in the TC is delayed fluorescence, which is quite slow compared to prompt fluorescence, the two can be easily distinguished. Therefore, the change in delayed fluorescence on anion coordination can be investigated, as can the rate of RISC. If the RISC and the profile of the delayed fluorescence do change on anion binding, this could give valuable sensing

information. Therefore, applying TADF to these systems could lead to more informative sensing materials, than their simply fluorescent counterparts.

SYNTHESIS

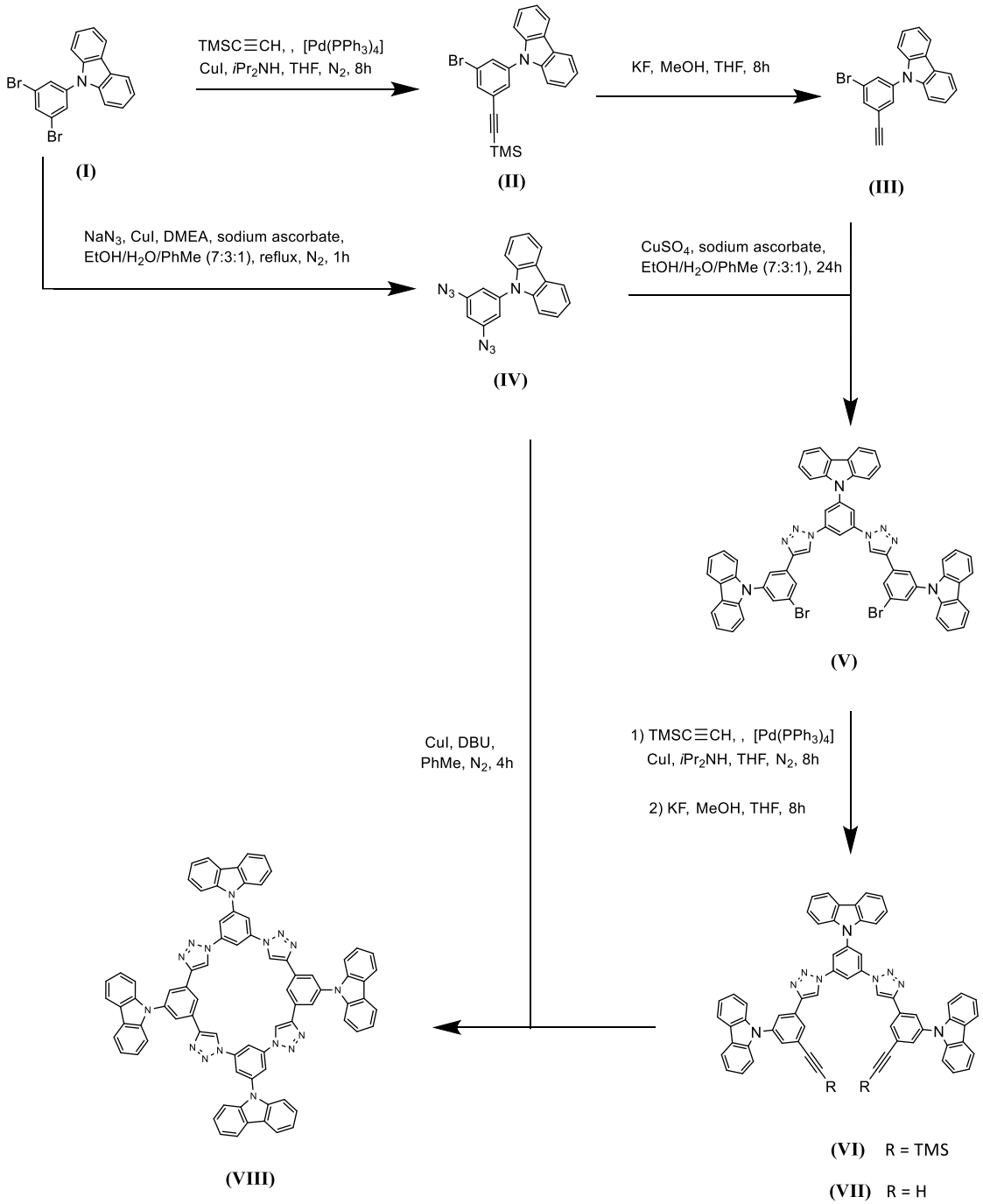

Synthetic route to target compound, all procedures are taken from literature[2]

*Preparation of **(II)***

Compound I (1 eq.), CuI (0.02 eq.), and $Pd(PPh_3)_2Cl_2$ (0.02 eq.) were placed in a two-neck flask, which was degassed under high vacuum and back-filled with argon three times. Degassed THF (50 mL) and $^{i}Pr_2NH$ (10 mL) were added followed by the dropwise addition of trimethylsilylacetylene (1 eq.). The reaction mixture was stirred for 8 hours at room temperature. The volatiles were removed *in vacuo* and the brown solid obtained was washed with water (3×30 mL), extracted with CH_2Cl_2 (2×50 mL), dried (Na_2SO_4) and concentrated under reduced pressure. The crude product was purified by column chromatography.

*Preparation of **(III)***

A 50 mL flask was charged with Compound II (1 eq.), KF (5 eq.), THF (10 mL) and methanol (10 mL) and stirred at room temperature for 8 hours. The volatiles were removed *in vacuo* and the solid obtained was extracted with CH_2Cl_2 (3×50 mL), washed with water (30 mL), dried (Na_2SO_4) and concentrated under reduced pressure. The crude product was purified by column chromatography.

*Preparation of **(IV)***

Compound I (1 eq.), NaN_3 (3 eq.), sodium ascorbate (0.1 eq.), CuI (0.2 eq.), N1,N2-dimethylethane-1,2-diamine (0.3 eq.) were added to the degassed solvent mixture EtOH:H_2O:toluene (7:3:1, 11 mL). The reaction mixture was stirred under reflux and the progress of the reaction was followed by TLC. When Compound I was completely consumed (after about 1 hour), the reaction mixture was allowed to cool to room temperature, and the crude mixture was purified by flash chromatography.

*Preparation of **(V)***

A solution of the Compound IV (1 eq.), and Compound III (2.2 eq.), sodium ascorbate (0.1 eq.), and $CuSO_4$ (0.01 eq.) in a 7:3:1 mixture of EtOH:H2O:toluene was stirred at room temperature for 24 hours. After removal of the solvents *in vacuo*, the crude product was purified by column chromatography.

*Preparation of **(VI)***

Compound V (1 eq.), CuI (0.12 eq.), and $Pd(PPh_3)_2Cl_2$ (0.12 eq.) were placed in a two-neck flask. The flask was degassed under high vacuum and back-filled with argon three times before the addition of degassed THF (10 mL), diisopropylamine (2 mL), followed by dropwise addition of trimethylsilylacetylene (2.4 eq.). The reaction mixture was stirred for 8 hours at room temperature. The volatiles were removed *in vacuo* and the brown solid obtained washed with water (3×30 ml), extracted with CH_2Cl_2 (2×50 ml), dried (Na_2SO_4) and concentrated under reduced pressure. The crude product was purified by column chromatography.

*Preparation of **(VII)***

A 50 mL flask was charged with Compound VI (1 eq.), KF (10 eq.), THF (10 mL) and methanol (10 mL) and stirred at room temperature for 8 hours. The volatiles were removed *in vacuo* and the solid obtained was extracted with CH_2Cl_2 (3×50 ml), washed with water (30 ml), dried (Na_2SO_4) and concentrated under reduced pressure. The crude product was purified by column chromatography.

*Preparation of **(VIII)***

DBU (20 eq.) was added to toluene (195 mL), and degassed with argon for 30 minutes and heated to 70 °C while flushing with argon. At 70 °C, CuI (0.3 eq.) was added to the mixture. A solution of Compound VII (1 eq.) and Compound IV (1 eq.) in dry toluene (50 mL) was added to the solution slowly over 10 hours and stirred for another 4 hours under argon. The mixture was then cooled to room temperature and filtered through a column of basic Al_2O_3, and the filtrate was concentrated *in vacuo*. The product was purified via flash chromatography.

RESULTS

Given the time constraints of the project, it was not possible to complete the entire synthesis as described by the literature procedures given above. Compounds II – IV were successfully synthesised and characterised by either gas chromatography-mass spectroscopy (GCMS), ^{1}H nuclear magnetic resonance (NMR) spectroscopy, ^{13}C DEPTQ NMR spectroscopy, or some combination of these, and the spectra have been included (see Supplementary Information). Purification of all compounds synthesised was difficult due to the very similar polarity of Br and the trimethylsilyl (TMS) group resulting in very similar R_f values, in many of the solvent systems tried.

Despite results given in the literature,[2] the catalyst $Pd(Ph_3)_2Cl_2$ did not appear to be active enough to promote the desired reaction. In lieu of this, $Pd(Ph_3)_4$ was used, as the lower oxidation state on the Pd in this complex is thought to make for a more active catalyst. Two different bases (Et_3N and $^{i}Pr_2NH$) were also screened, with the latter giving a higher yield of the mono-coupled product, according to peak integral estimations from GCMS (63% vs. 61%) and a lower yield of the di-coupled product (3% vs. 5%). The formation of the cross-coupled Compound II expected from the Sonogashira conditions used was reflected by the shifts in the ^{1}H NMR (δ_H = 7.70, 7.61 and 0.26 ppm), which were consistent with values reported in the literature,[2] for the ^{t}Bu analogue of Compound II (relevant signals at δ_H = 7.64, 7.43 and 0.25 ppm). The molecular ion peak was also observed in the GCMS at the expected m/z value. As well as the desired mono-coupling product (prepared in 47% yield), TLC analysis demonstrated the formation of a side product, which was ascribed to competing di-substitution. This was reflected in the NMR and GCMS spectra. The formation of the disubstituted analogue of Compound II accounted for approximately 10% of the starting Compound I. The low yield of both coupling reactions could be a result of the reaction vessel having not been fully purged of oxygen and water before the reaction was carried out. The bis(trimethylsilyl)ated product was easily identifiable by NMR, given the large integration value and very low chemical shift of the protons in the two equivalent TMS groups. By comparison of the ^{1}H NMR of the mono and di-coupled products, the increase in symmetry can be inferred from a simplification of the spectrum in the aromatic region, as two chemically inequivalent protons in Compound II collapse into one signal in the di-coupled case, as shown in *Figure 6*. The number of C-H and quaternary C signals in the ^{13}C DEPTQ NMR of the dicoupled product reinforces the presence of the expected alkyne, particularly distinctive are the quaternary signals at δ_C = 53.6 ppm and 96.7 ppm, which represent the two C atoms in the triple bond.

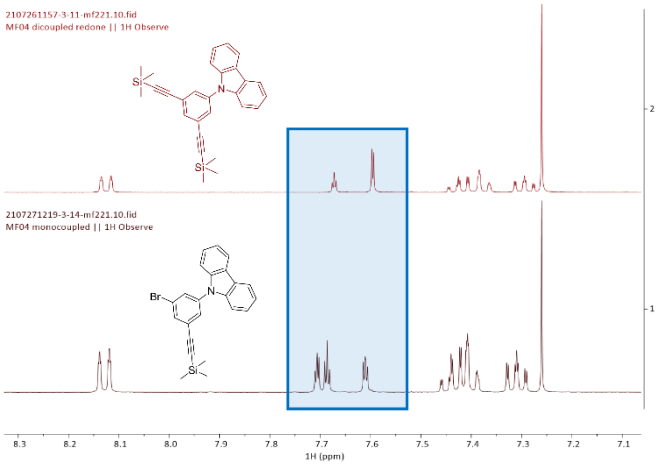

Figure 6: Aromatic regions of NMR of mono and di-coupled products

The deprotection of the silylated alkynes proceeded with high yields (86% and 90% for Compound II and its di-coupled analogue, respectively), as expected, however it should be mentioned that on workup of Compound III, some of the product was spilled in the fumehood. The appearance of an additional proton environment (at approximately δ_H = 3.2 ppm) for both the mono and di-coupled products, with the expected integration values, leaves little doubt that the corresponding alkynes were formed.

From Compound V onwards, the molecular weights became too large for reliable analysis by GCMS, so characterisation became more difficult. However, the first attempt of click chemistry between Compound III and Compound IV to form the triazole-bearing Compound V was unsuccessful as shown by the stacked ^{1}H NMR (*Figure 7)*. The spectrum of the reaction mixture and that of the starting alkyne (*Figure 7a*) are almost identical, and the few additional peaks present in the spectrum of the reaction mixture that are not present for the starting alkyne can be seen in the spectrum of the diazide (*Figure 7b*). This clearly indicates no reaction took place.

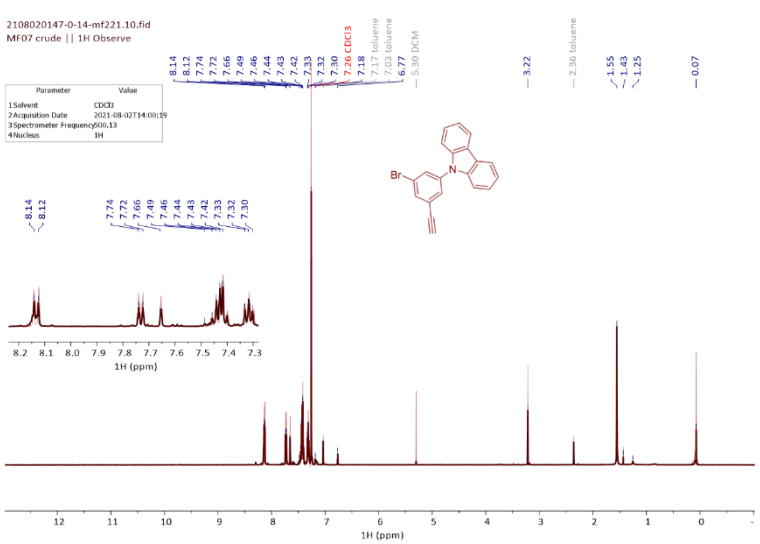

Figure 7a: Stacked NMR spectra of alkyne (brown) and click chemistry reaction mixture (black)

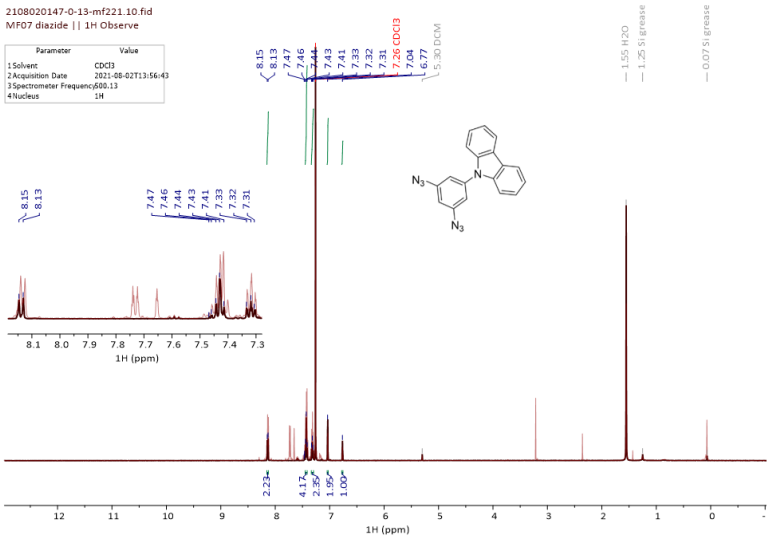

Figure 7b: Stacked NMR spectra of click chemistry reaction mixture (brown) and diazide (black)

Given the reputation of click chemistry for near-quantitative yields, explanations were sought to explain this, and it was suggested that the thermodynamic instability of Cu(I) in aqueous media necessitates a good ligand to stabilise it.[9] A common ligands used is tris[(1-benzyl-1H-1,2,3-triazol-4-yl)methyl]amine (TBTA), however this was unavailable, so the reactions between Compound III and phenylazide, as well as the di-coupled version of Compound III and phenylazide were conducted under the same click conditions as above, with the ratios of ethanol: water: toluene changed from 7:3:1 to 5:3:3, and with the addition of diisopropylethylamine (3.5 eq.). More encouraging results were seen in the ^{1}H NMR, as shown in *Figure 8*. The increase in complexity of the aromatic region, and the appearance of more deshielded proton environments at higher chemical shifts for both the mono and di-coupled compounds could be an indicator of the desired electron poor C-H bonds in the triazole ring. These structures are supported by the integration values on the ^{1}H NMR spectra (see Supplementary Information).

By comparing the ^{1}H NMR spectra of the triazole with the bis(triazole), the strong negatively inductive electron withdrawing effect of the N atoms manifests as a downfield shift in some of the signals. Particularly interesting is the shift of the alkene C-H bond in the triazole (δ_H = 8.25 ppm) versus the bis(triazole) (δ_H = 8.37 ppm), as shown in blue on *Figure* 8. The symmetry of the latter compound results in an increase in the integration value of the protons in this environment, and the downfield shift is consistent with a more electron deficient molecule. The multiplicity of this signal (singlet) also reinforces this assignment. Furthermore, the only signal that integrates to 1 left in the bis(triazole) is

significantly more deshielded (δ_H = 8.56 ppm) compared with the triazole (δ_H = 7.69 ppm), owing to the adjacency of 2 highly electron withdrawing groups, explaining the large shift in the position of this

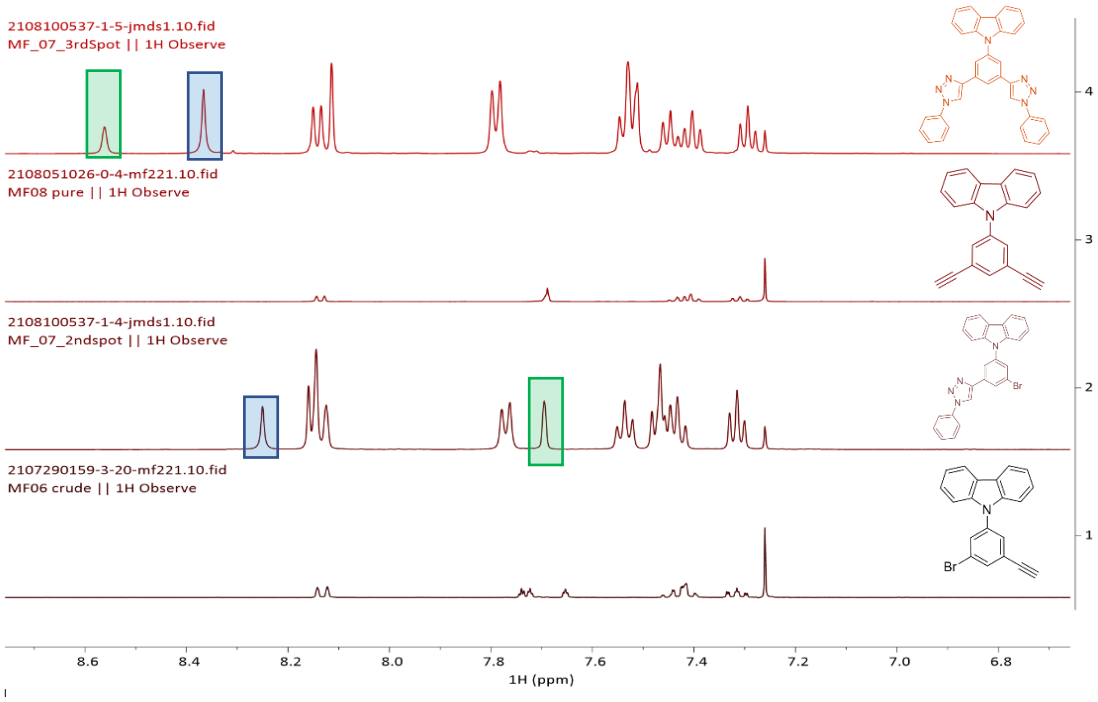

Figure 8: Stacked NMR spectra of the products of repeated click reaction with EtN(^{i}Pr)$_2$ added (3.5 eq.)

signal (shown in green on *Figure 8*). This demonstrates the importance of a Cu(I) ligand to the success of click chemistry and would have been incorporated in the next attempt of the reaction if more time were available. Many of the signals appear at very similar chemical shifts in both the triazole and bis(triazole), indicating that the electron withdrawing effect is relatively localised.

Similarly, the ^{13}C DEPTQ NMR spectra indicate the desired click reaction was successful. In the molecule bearing a single triazole unit, all the expected signals were observed. Both the ^{13}C and ^{1}H NMR suggest that there is still some trace of the starting alkyne Compound III, given the diagnostic alkyne peaks still present (δ_C ~ 80 ppm and δ_H = 3.23 ppm). The peak heights help to, crudely, identify which C environments are responsible for which signals. Given the symmetry in the carbazole and phenyl subunits places more than one C atom in the same environment, it is a reasonable assumption that the largest peaks in the aromatic region can be attributed to these C atoms. The lack of directly bound protons at quaternary C atoms remove an important relaxation pathway for ^{13}C nuclei, resulting in signals with very low intensities, that can be distinguished based on their local environments. For example, those directly bound to N atoms appear furthest downfield, whilst the Br-bound quaternary C appears at a slightly lower chemical shift.

In the bis(triazole), the symmetry of the molecule aids in understanding its ^{13}C NMR spectrum, as this reduces the number of C environments by two. The number of signals with the correct orientations are consistent with expectation. By comparing the rough peak areas with that of the single triazole species, certain peaks can be characterised. For example, the signals at δ_C = 118.52 ppm, 124.78 ppm and 129.14 ppm in the mono(triazole), roughly double in area in the bis(triazole) spectrum. These must therefore be attributable to the C atoms 8, 11 and 15 in *Figure 9*, as the populations of these environments also double in the bis(triazole). These can be seen in *Figure 10* in the blue boxes. Given the electron deficiency of C environment 11, the most deshielded signal (δ_C = 129.14 ppm) has been assigned to this. The largest peaks (δ_C = 129.95 ppm and 120.56 ppm) in the aromatic region of the bis(triazole) can be trivially assigned

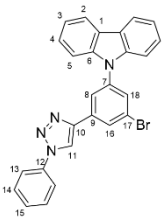

Figure 9: Click product of using alkyne and PhN$_3$

to the equivalent protons in the phenyl substituents, based off an estimation from the peak areas, as shown in the orange boxes of *Figure 10*. The increase in integration of the quaternary C at δ_C = 132.94 ppm in the bis(triazole) vs. its monosubstituted analogue suggests this is attributable to the N-bound C in the phenyl ring (shown in green). The disappearance of the quaternary C signal at δ_C = 123.63 ppm (yellow) and the C-H signal at δ_C = 130.19 ppm (purple) reinforces the symmetry imposed on di-coupling, as these were originally attributed to the C bound to Br and the C-H bond *ortho* to the C-Br, respectively. The peak corresponding to the electron deficient quaternary C in the triazole ring (red) appears at a similar shift in both compounds, and the increase in signal intensity matches expectation.

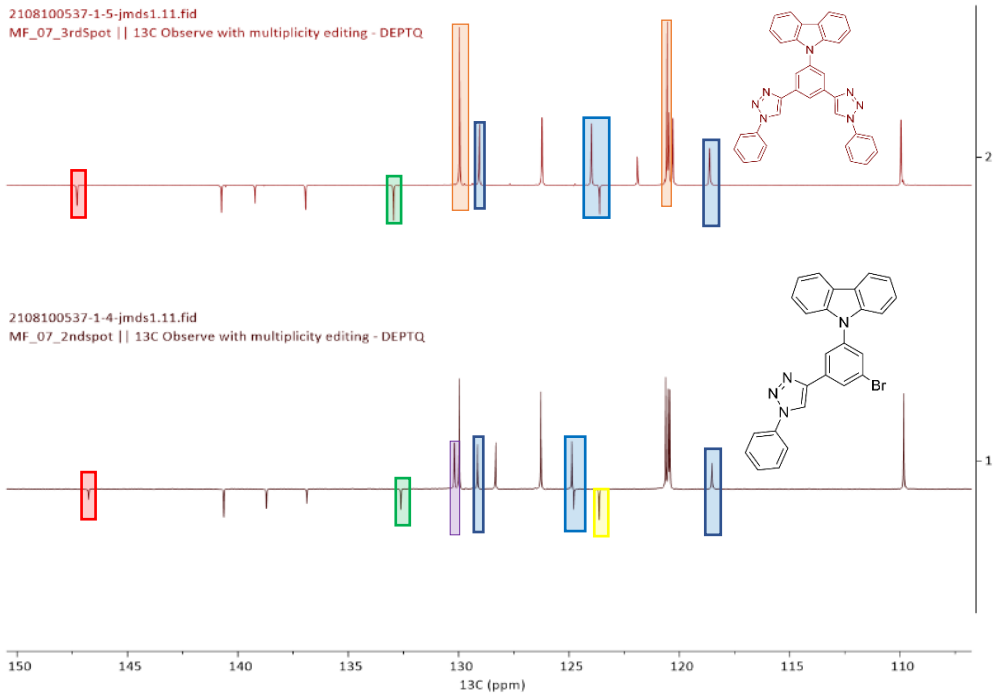

Figure 10: Stacked NMR of triazole and bis(triazole)

CONCLUSION

A new macrocycle, inspired by literature[2], expected to be capable of strong anion binding (without the need for classical hydrogen bonds) was computationally predicted to be TADF active using the PBE0/6-31G(d,p) method. Intermediates to this macrocycle (Compounds II-IV) were successfully synthesised, with varying yields, and purified according to procedures given in the literature.[2] Concurrently, the di-coupled versions of Compound II and Compound III were also synthesised. The expected structures were supported by the spectroscopic data recorded, and a procedure for successful click reaction without the need for TBTA was also found.

FUTURE WORK

The remainder of the synthesis should be completed according to the relevant procedures, the photophysical properties and anion (halide) binding competence of the TC should be measured to assess the viability of applying TADF to this macrocyclic anion receptor. By varying the substituents and size of the central cavity, complexation with other molecules could also be investigated.

ACKNOWLEDGEMENTS

I am grateful to Professor Zysman-Colman as well as the Zysman-Colman group for welcoming me so warmly and for supplying such an interesting project. Given the ever-evolving nature and countless logistical delays precipitated by the Covid-19 pandemic, I must stress my thanks to Professor Zysman-Colman for ensuring my research experience remained as valuable and stimulating as ever. For his enduring patience and guidance, I must also commend Dr John Marques Dos Santos; without his supervision I wouldn't have managed to make as much progress in the few weeks in the lab as I did. I wish him the best as he continues with the project. Finally, this experience was only possible given the generous funding of Lord Laidlaw of Rothiemay and the Laidlaw Scholarship, to whom I am deeply thankful for both my personal and academic development.

REFERENCES

[1] P. A. Gale, E. N. W. Howe and X. Wu, *Chem*, 2016, **1**, 351-422.
[2] Y. Li and A. H Flood, *Angew. Chem. Int. Ed.*, 2008, **47**, 2649-2652.
[3] V. S. Bryantsev and B. P. Hay, *J. Am. Chem. Soc.*, 2005, **127**, 8282-8283.
[4] D. J. Cram, *Angew. Chem. Int. Ed. Engl.*, 1988, **27**, 1009-1020.
[5] M. Kasha, *Discuss. Faraday Soc.*, 1950, **9**, 14-19.
[6] Z. Yang, Z. Mao, Z. Xie, Y. Zhang, S. Liu, J. Zhao, J. Xu, Z. Chi and M. P. Aldred, *Chem. Soc. Rev.*, 2017, **46**, 915.
[7] C. Adachi, *Jpn. J. Appl. Phys.,* 2014, **53**, 060101.
[8] J. B. Xiong, J. H. Wang, B. Li, C. Zhang, B. Tan and Y. S. Zheng, *Org. Lett.*, 2018, **20**, 321-324.
[9] T. R. Chan, R. Hilgraf, K. B. Sharpless and V. V. Fokin, *Org. Lett.*, 2004, **6**, 2853-2855.

SUPPLEMENTARY INFORMATION

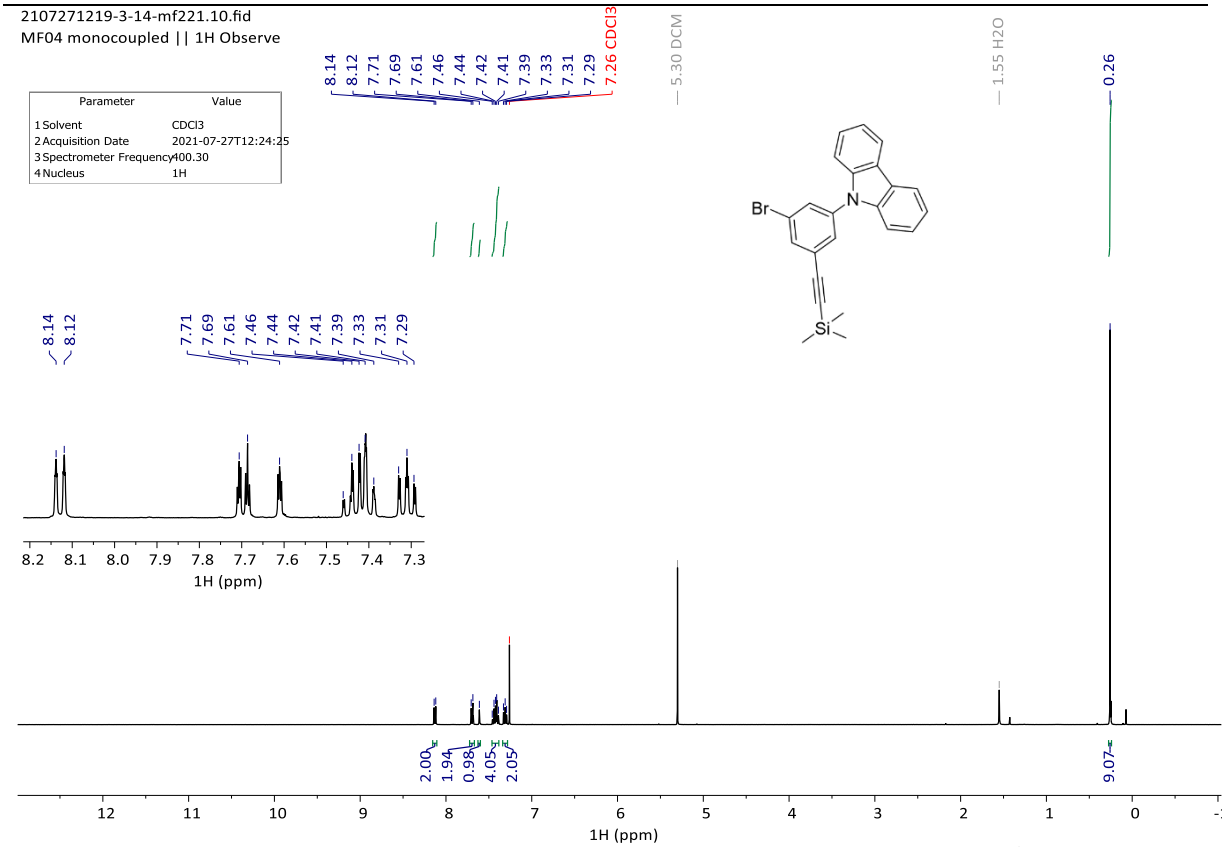

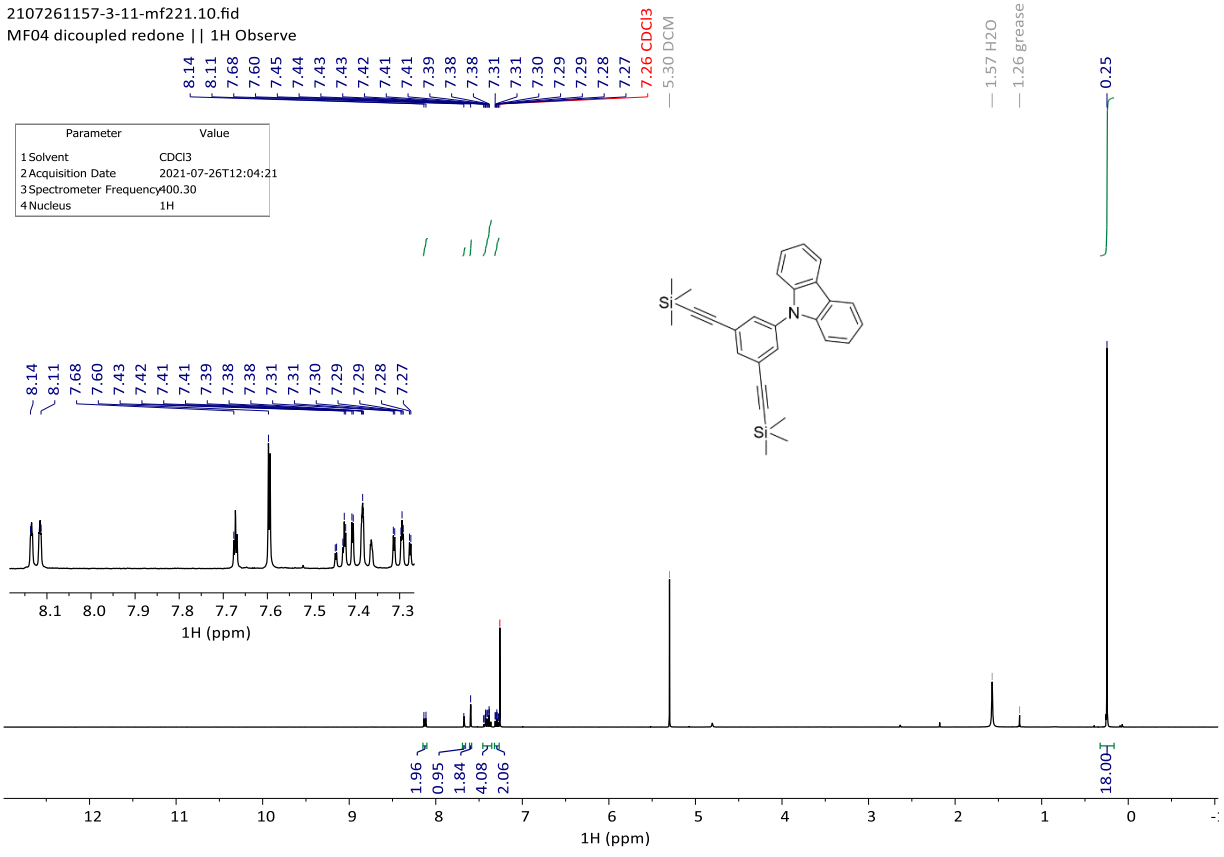

2107260126-3-19-mf221.10.fid
MF04 dicoupled || 13C Observe with multiplicity editing - DEPTQ

Parameter	Value
1 Solvent	CDCl3
2 Acquisition Date	2021-07-26T19:51:23
3 Spectrometer Frequency	100.67
4 Nucleus	13C

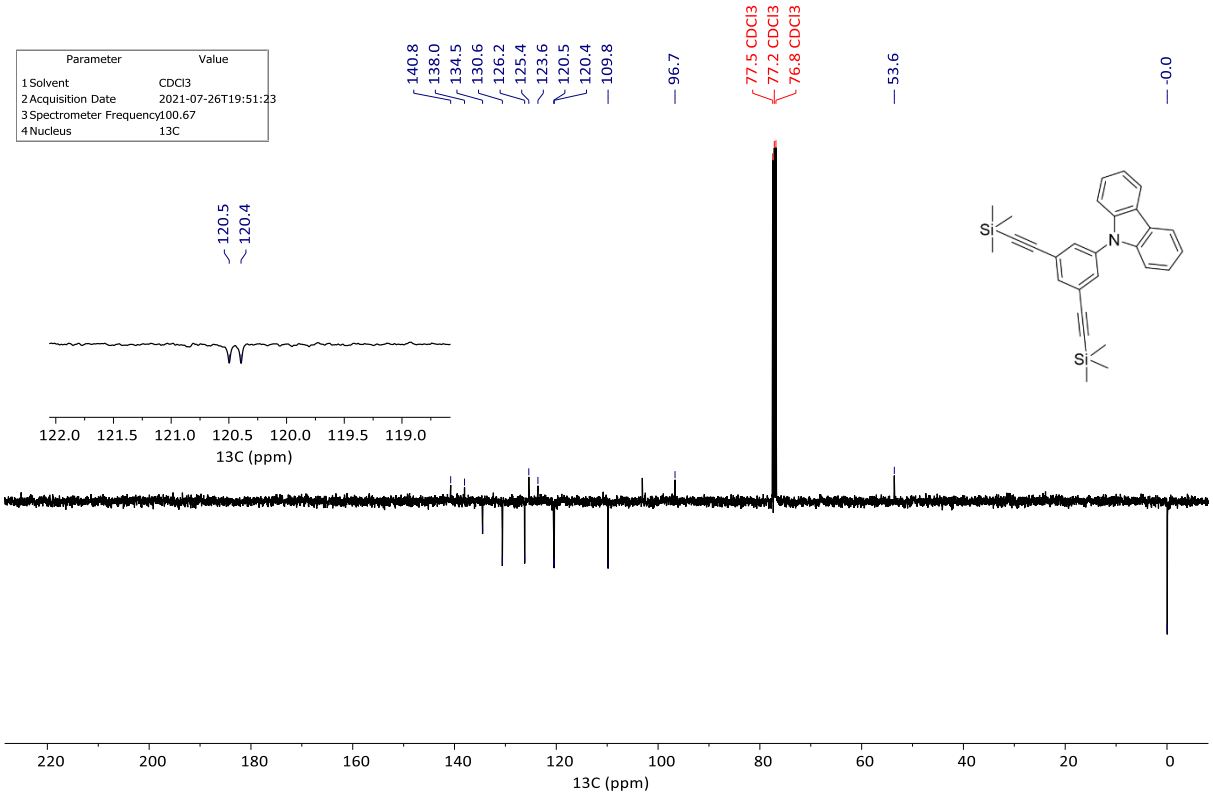

2107290159-3-20-mf221.10.fid
MF06 crude || 1H Observe

Parameter	Value
1 Solvent	CDCl3
2 Acquisition Date	2021-07-29T14:08:47
3 Spectrometer Frequency	400.30
4 Nucleus	1H

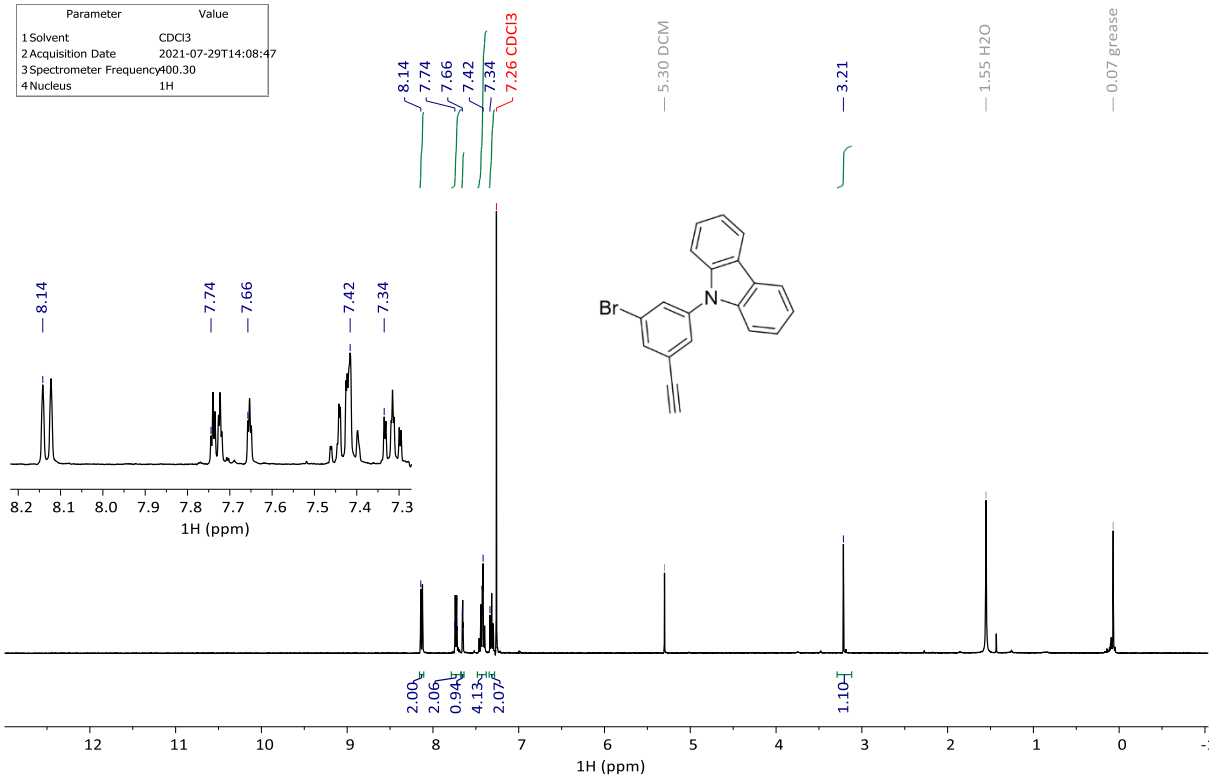

2107290159-3-20-mf221.10.fid
MF06 crude || 1H Observe

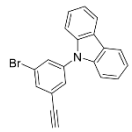

2108020147-0-14-mf221.10.fid
MF07 crude || 1H Observe

2108020147-0-13-mf221.10.fid
MF07 diazide || 1H Observe

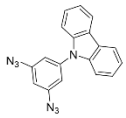

2108051026-0-4-mf221.10.fid
MF08 pure || 1H Observe

Parameter	Value
1 Solvent	CDCl3
2 Acquisition Date	2021-08-05T10:32:41
3 Spectrometer Frequency	500.13
4 Nucleus	1H

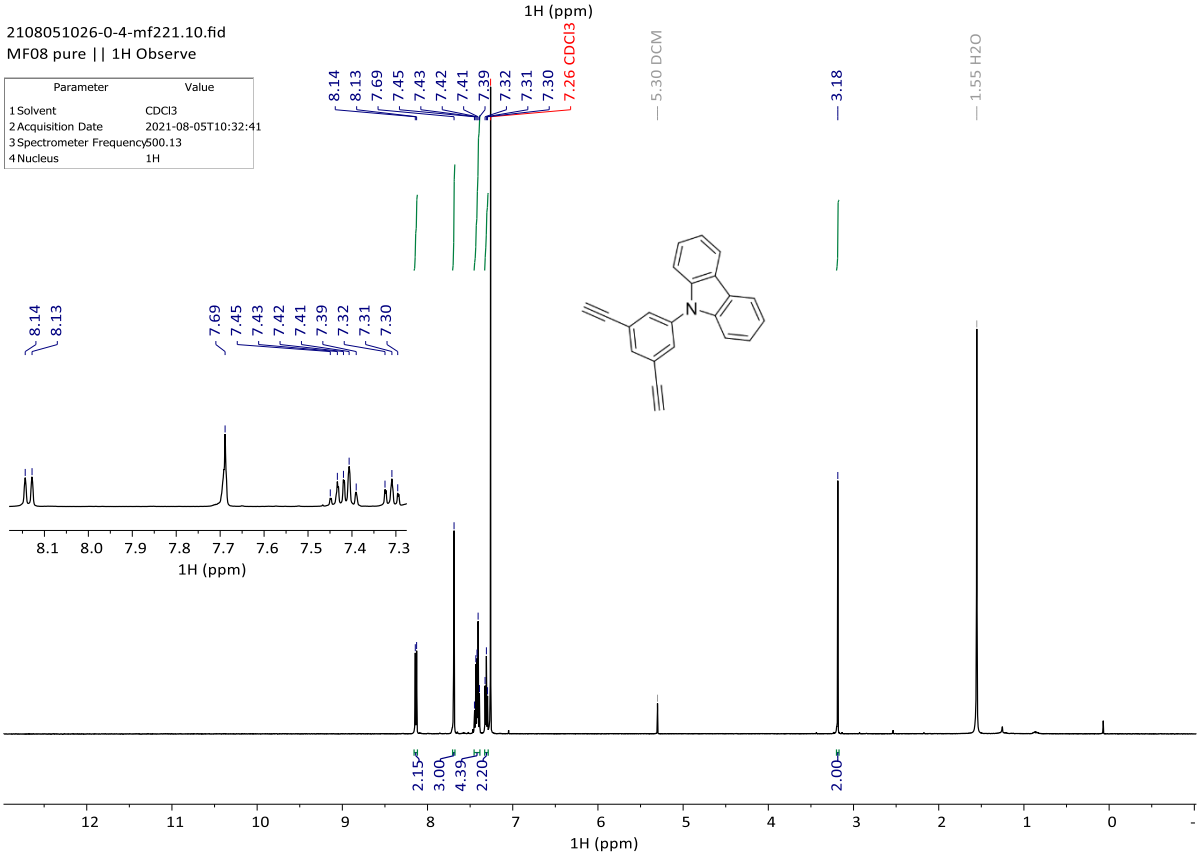

2108100537-1-4-jmds1.10.fid
MF_07_2ndspot || 1H Observe

Parameter	Value
1 Solvent	CDCl3
2 Acquisition Date	2021-08-10T21:35:06
3 Spectrometer Frequency	499.93
4 Nucleus	1H

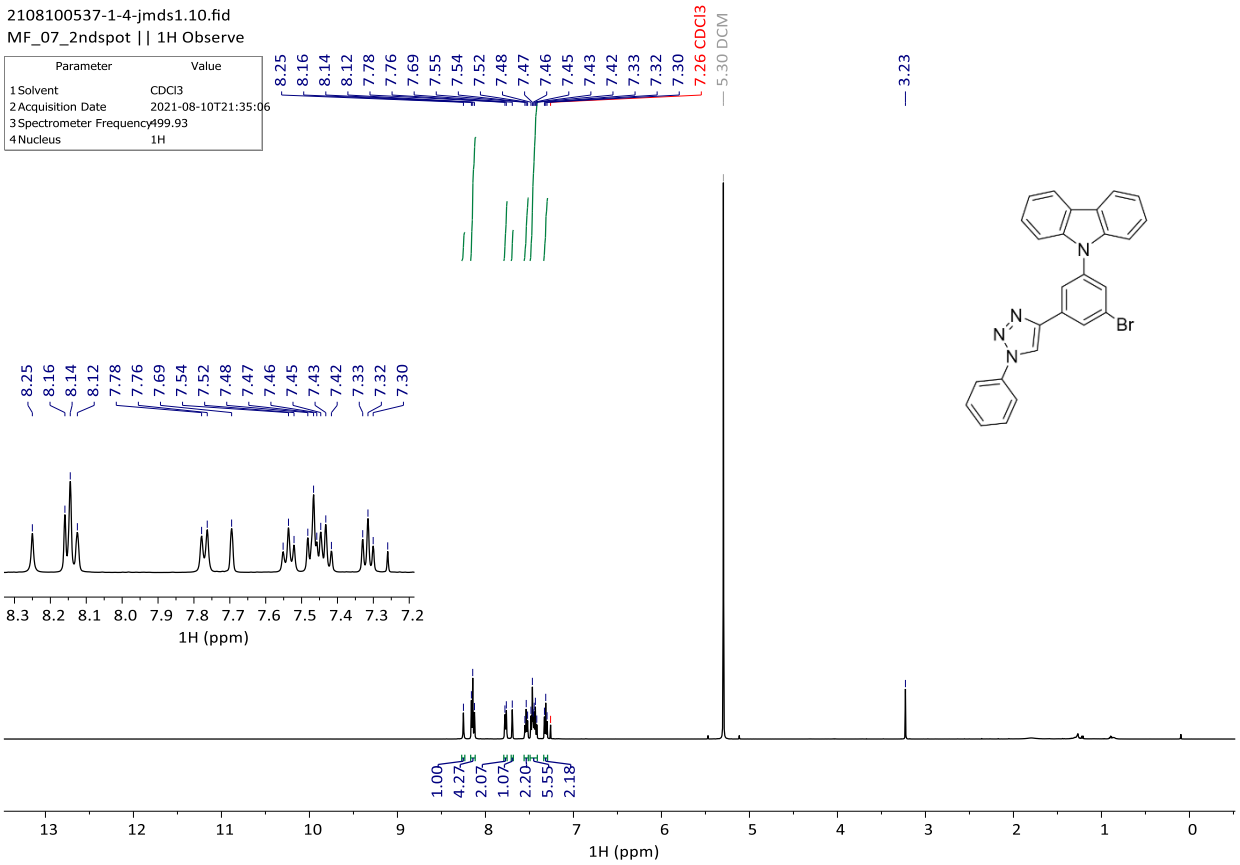

2108100537-1-5-jmds1.10.fid
MF_07_3rdSpot || 1H Observe

Parameter	Value
1 Solvent	CDCl3
2 Acquisition Date	2021-08-10T23:00:13
3 Spectrometer Frequency	499.93
4 Nucleus	1H

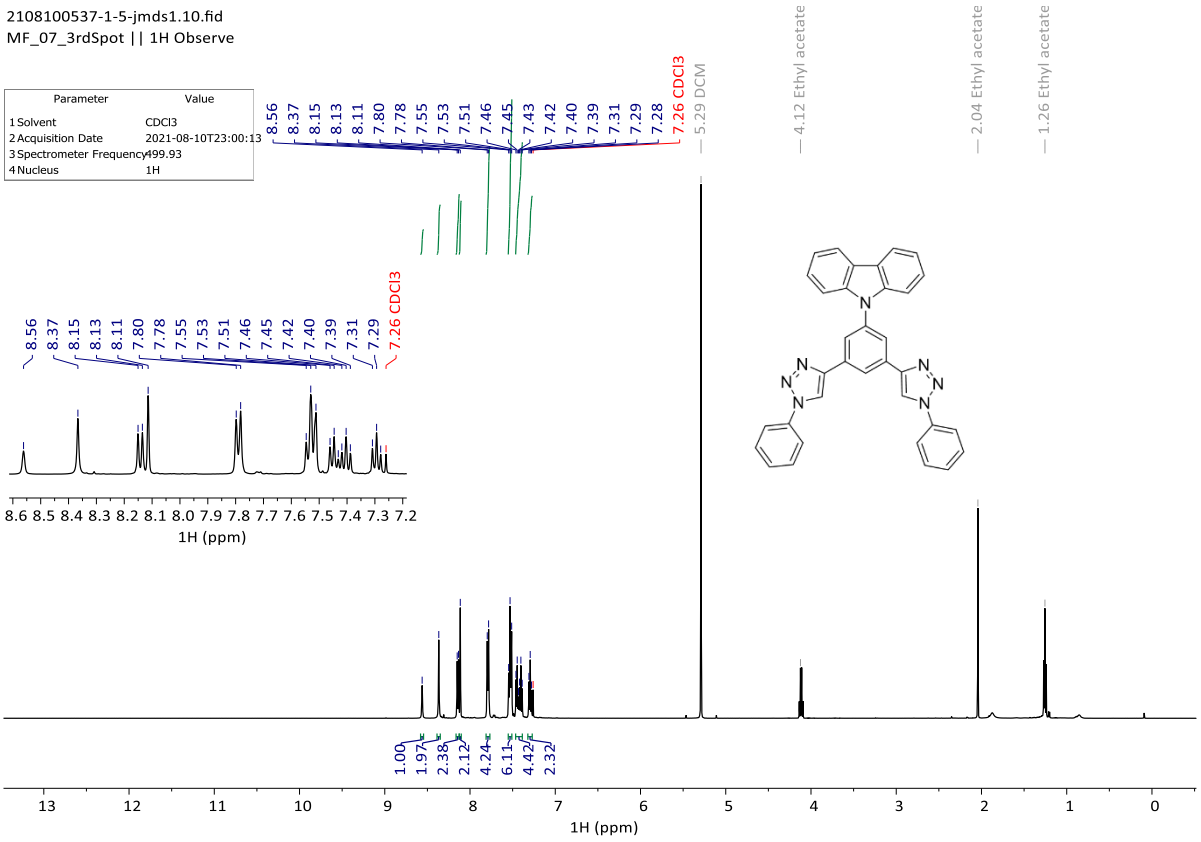

2108100537-1-4-jmds1.11.fid
MF_07_2ndspot || 13C Observe with multiplicity editing - DEPTQ

Parameter	Value
1 Solvent	CDCl3
2 Acquisition Date	2021-08-10T22:54:58
3 Spectrometer Frequency	125.72
4 Nucleus	13C

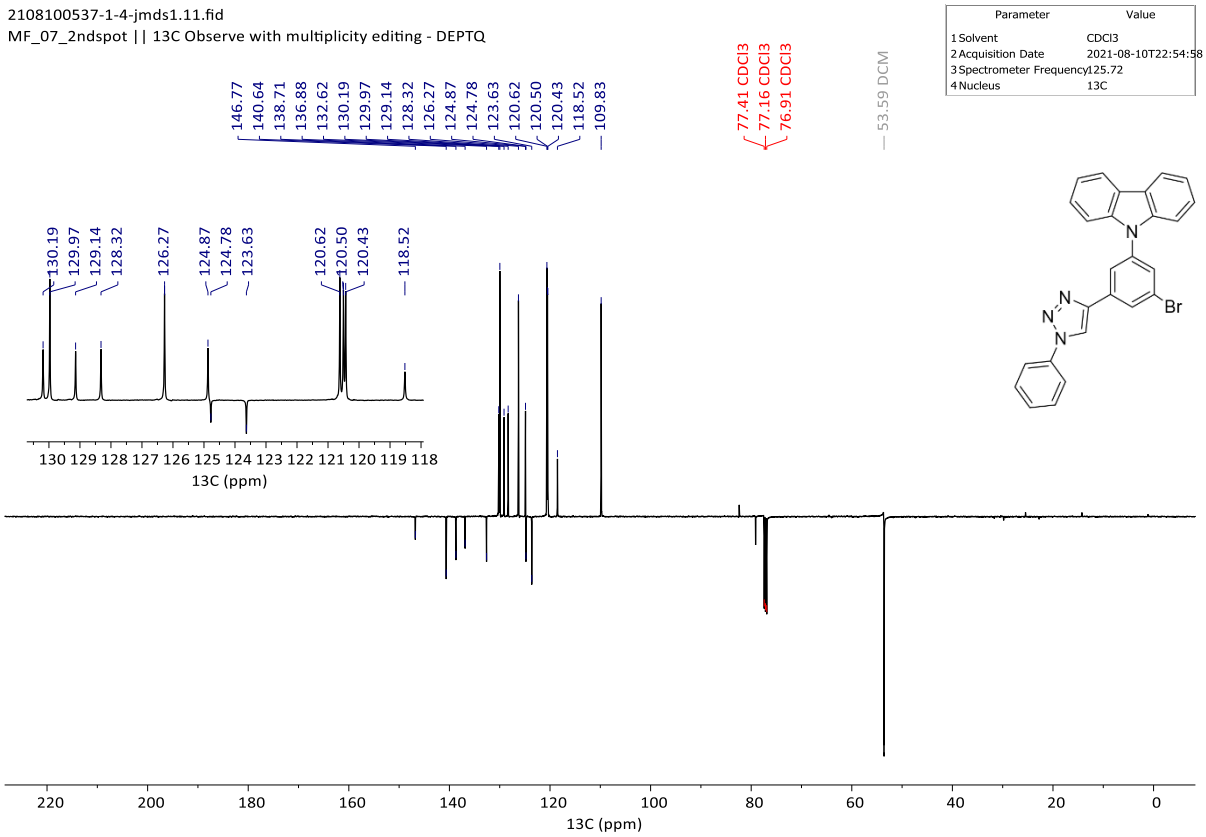

2108100537-1-5-jmds1.11.fid
MF_07_3rdSpot || 13C Observe with multiplicity editing - DEPTQ

Parameter	Value
1 Solvent	CDCl3
2 Acquisition Date	2021-08-11T00:20:05
3 Spectrometer Frequency	125.72
4 Nucleus	13C

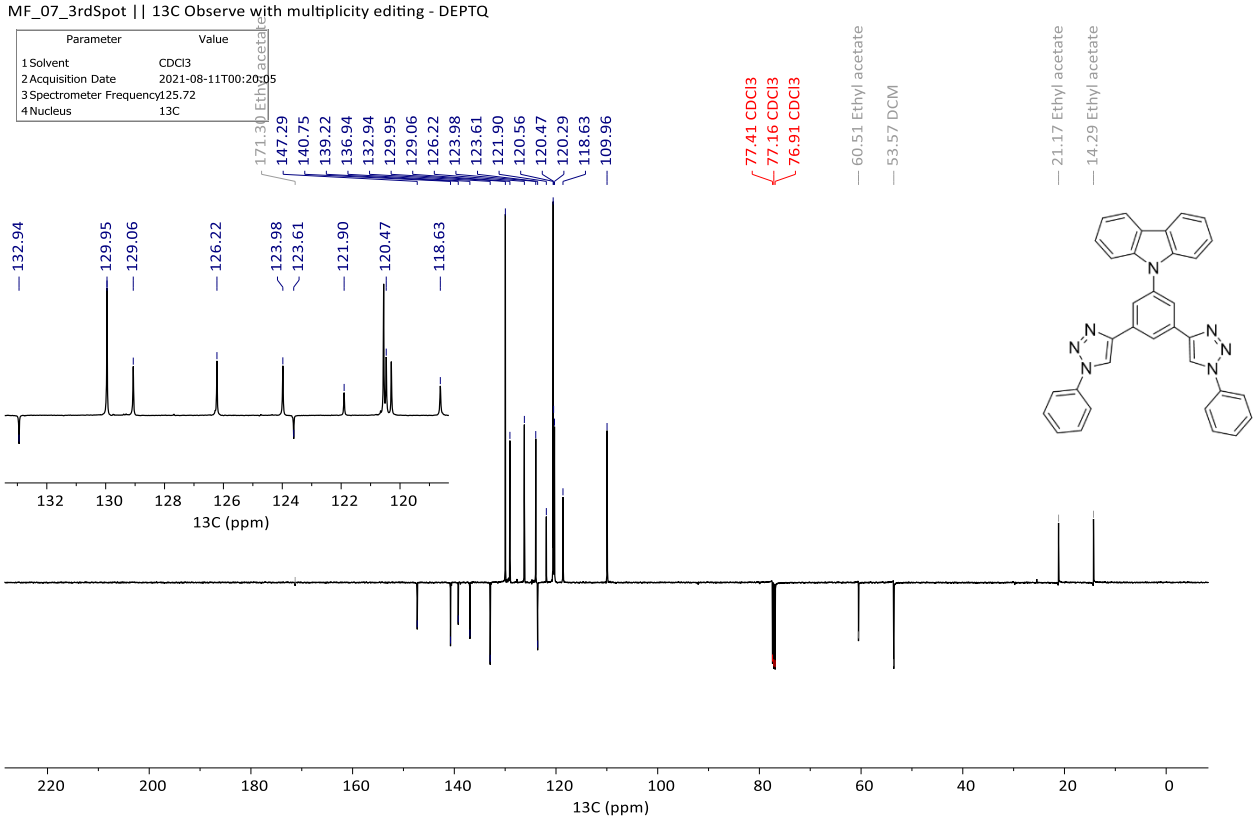

Line#:1 R.Time:12.458(Scan#:1136)
MassPeaks:583
RawMode:Single 12.458(1136) BasePeak:417.10(577631)
BG Mode:None Group 1 - Event 1 Scan

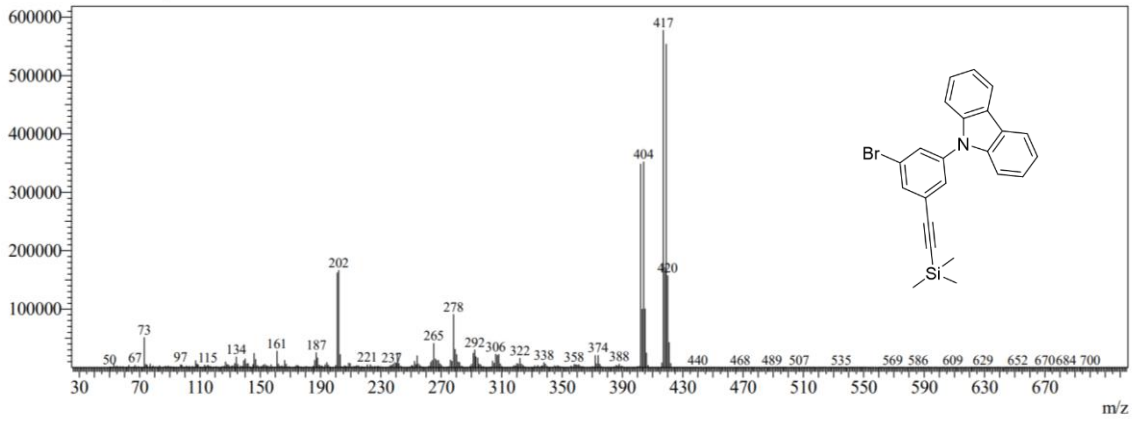

Line#:1 R.Time:13.175(Scan#:1222)
MassPeaks:590
RawMode:Single 13.175(1222) BasePeak:435.25(154327)
BG Mode:None Group 1 - Event 1 Scan

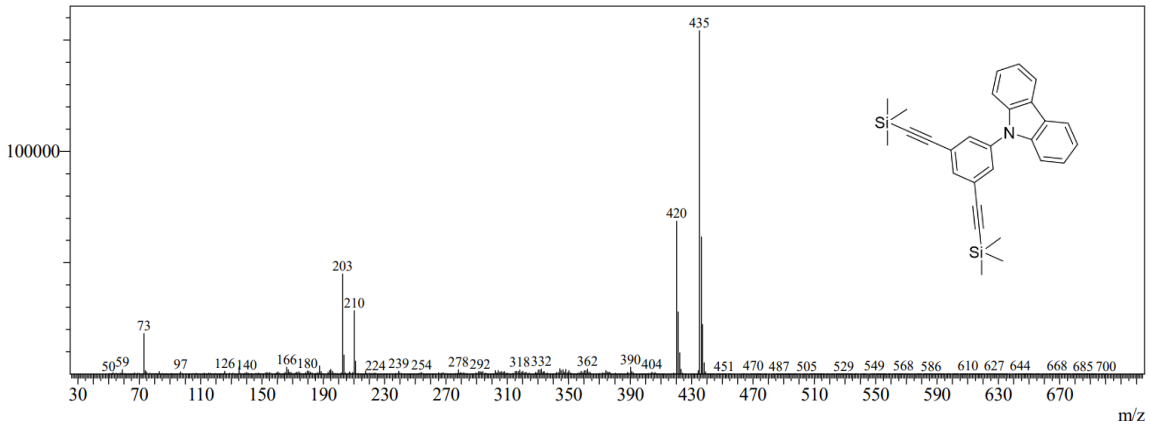

Line#:1 R.Time:11.217(Scan#:987)
MassPeaks:629
RawMode:Single 11.217(987) BasePeak:345.05(1137915)
BG Mode:None Group 1 - Event 1 Scan

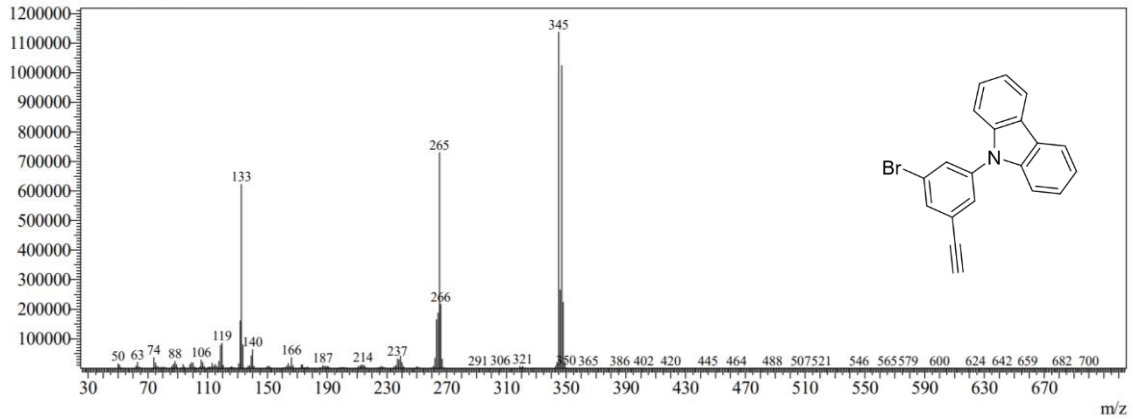

Line#:1 R.Time:10.733(Scan#:929)
MassPeaks:547
RawMode:Single 10.733(929) BasePeak:291.20(1197446)
BG Mode:None Group 1 - Event 1 Scan